

RSC Advances



This is an *Accepted Manuscript*, which has been through the Royal Society of Chemistry peer review process and has been accepted for publication.

Accepted Manuscripts are published online shortly after acceptance, before technical editing, formatting and proof reading. Using this free service, authors can make their results available to the community, in citable form, before we publish the edited article. This *Accepted Manuscript* will be replaced by the edited, formatted and paginated article as soon as this is available.

You can find more information about *Accepted Manuscripts* in the [Information for Authors](#).

Please note that technical editing may introduce minor changes to the text and/or graphics, which may alter content. The journal's standard [Terms & Conditions](#) and the [Ethical guidelines](#) still apply. In no event shall the Royal Society of Chemistry be held responsible for any errors or omissions in this *Accepted Manuscript* or any consequences arising from the use of any information it contains.

1 **Effect of air-gap length on Carbon dioxide stripping performance of**
2 **surface modified Polysulfone hollow fiber membrane contactor**

3
4 **M. Rahbari-Sisakht^{a,b}, F. Korminouri^a, D. Emadzadeh^{a,b}, T. Matsuura^c and**
5 **A.F. Ismail^{a,*}**

6 ^a Advanced Membrane Technology Research Center (AMTEC), Universiti Teknologi Malaysia (UTM), 81310 Skudai, Johor,
7 Malaysia

8 ^b Department of Chemical Engineering, Gachsaran Branch, Islamic Azad University, Gachsaran, Iran

9 ^c Department of Chemical and Biological Engineering, University of Ottawa, 161 Louis Pasteur St., Ontario K1N 6N5, Canada

10
11 *Corresponding author: Tel.: +60 75535592; Fax: +60 75535925. E-mail addresses: afauzi@utm.my and
12 fauzi.ismail@gmail.com.

13
14
15 **ABSTRACT**

16 Surface Modifying Macromolecule (SMM) blended PSf hollow fibers were spun at different air-
17 gaps to evaluate CO₂ stripping from aqueous DEA solution and water. The fabricated membranes
18 were firstly subjected to different characterization methods such as contact angle and liquid entry
19 pressure measurement to evaluate the membrane's hydrophobicity and wetting resistance,
20 respectively. To determine pore size and effective porosity of the membranes, the pure helium
21 permeation test was performed. Morphological study of the membranes was conducted by
22 scanning electron microscopy (SEM) and atomic force microscopy (AFM). CO₂ stripping test
23 was carried out to investigate the effects of operating variables such as liquid and gas velocity,
24 temperature and DEA concentration on CO₂ stripping flux. It was found that the increase of
25 liquid velocity resulted in enhanced CO₂ stripping flux. On the other hand, the increase in gas
26 velocity did not exert significant influence on the stripping flux. The increase in temperature and
27 DEA concentration both enhanced the stripping flux. Lastly, it was concluded that the hollow
28 fiber spun in this work at 15 cm air-gap could achieve the best stripping flux among all the
29 membranes fabricated so far for the CO₂ stripping.

30

31 **Keywords:** Polysulfone hollow fiber membrane; CO₂ stripping; membrane contactor; air-gap
32 length.

33 **1. Introduction**

34 Capture and removal of carbon dioxide (CO₂), the main greenhouse gas, from fossil fuel
35 combustion is arguably the most critical environmental concern worldwide. More than 80% of
36 industrial and domestic energy utilization are provided by fossil fuels and contribute significantly
37 to escalation of atmospheric CO₂ levels, which results inevitably in increase of significant
38 climate change.¹A technology for CO₂ removal from gas flows is hence required. Several
39 techniques are presently applied to separate CO₂ from gas streams using various chemical and
40 physical processes including absorption, adsorption, cryogenic and membranes.²⁻¹¹The
41 conventional technologies for CO₂ capture face some operational downsides for instance,
42 flooding, foaming and weeping, which can adversely influence performance and costs of power
43 stations. Hollow fiber membrane (HFM) contactor is an energy and cost efficient technology,
44 which can be applied for depletion of CO₂ from a variety of industrial process gas streams. HFM
45 contactor is a modular and flexible device with a high contact area for liquid and gas phase and
46 high mass transfer rate per unit volume. Due to the noticeable advantages of HFM contactors, in
47 recent years there is an increasing acceptance to use this technology for gas separation.¹²⁻²¹. The
48 major challenge of using HFs is membrane wettability which results in escalation of mass
49 transfer resistance and reduction of CO₂ flux. To prevent membrane wetting hydrophobic
50 polymers should be chosen.

51
52 Polysulfone (PSf) has been used for a long time as a polymeric material for HFM
53 preparation. This polymer, according to Rahbari-Sisakht *et al.*²² despite not being highly
54 hydrophobic can be a surpassing option for membrane fabrication due to its great thermal and
55 mechanical endurance and high solubility in the solvents. To elevate the hydrophobicity of
56 membrane surface, blending surface modified macromolecules (SMM) in the polymer dope can
57 be a favored method. SMM is an amphipathic macromolecule consisting of hydrophilic and
58 hydrophobic parts. In a polymer blend, thermodynamic incompatibility between polymers
59 usually causes demixing of polymers to occur. If the polymer system is equilibrated in air, the
60 polymer with the lowest surface energy will concentrate at the air interface and reduce the

61 system's interfacial tension as a consequence.²³ In our previous work, EDX results showed that
62 during hollow fiber spinning, SMM tends to migrate to membrane – air surface and changes the
63 membrane outer surface properties.²⁴ The SMM surface migration occurs during membrane
64 fabrication process due to the difference in energy levels of the SMM and base polymer, which
65 leads to improve hydrophobicity of the HF surface. The detailed kinetics and mechanism of
66 SMM surface migration is presented in earlier study.²⁵ The air-gap is one of the principal
67 spinning conditions that affects the amount of migrated SMM to the membrane-interface by
68 providing a sufficient amount of time for SMM migration. The study into the effect of air-gap on
69 membrane performance and structure has been conducted over the past few decades for various
70 separation processes.²⁶⁻³⁶

71
72 MC systems have a considerable potential to regenerate or desorb the absorbent solution.
73 In the absorption process, unwanted gas (CO₂) is absorbed by the liquid absorbent. In the
74 regeneration procedure, on the other hand, desorption of CO₂ takes place. The liquid absorbent is
75 in contact with one end of the HFM pore and CO₂ diffuses through the pore, and stripped by the
76 stripping gas at the other end of the pore to regenerate the liquid absorbent.

77
78 Many studies have focused on the absorption unit using HFMcontactors,³⁷⁻³⁹ while only a
79 few works have been carried out until now on CO₂ stripping through MCs. Recently, a research
80 has been done by Khaisri *et al.*⁴⁰ to strip CO₂ from monoethanolamine (MEA) solution using
81 polytetrafluoroethylene (PTFE)HFM. They concluded that the stripping efficiency was elevated
82 with the increase of the liquid velocity, operating temperature and absorbent concentration. On
83 the other hand, the gas side mass transfer resistance did not deeply affect the CO₂ desorption
84 flux. Kumazawa⁴¹ conducted a study on CO₂ desorption from 2-amino-2-methyl-1-propanol
85 (AMP) through PTFE membrane. They found that desorption process is ascribed to diffusion and
86 chemical reaction in the liquid side. They concluded that an increase in concentration of AMP
87 and the loaded CO₂ in the solution resulted in enhancement of total mass transfer coefficient.
88 Naim *et al.*⁴² produced PVDF membrane to strip CO₂ from aqueous diethanolamine (DEA)
89 solution. They added LiCl in the polymer solution as an additive to investigate the effect of
90 different LiCl levels on stripping performance of the membrane. A linear increase in stripping
91 flux was observed with increasing LiCl concentration. A study by Mansourizadeh and Ismai⁴³

92 focused on CO₂ stripping from water using PVDF membrane. Their results showed that the
 93 increase of inlet liquid concentration led to increase of CO₂ stripping performance. Rahbari-
 94 Sisakht *et al.*⁴⁴ fabricated PVDF fibers modified by SMM to strip CO₂ from diethanolamine
 95 solution. Their experimental found that the CO₂ desorption flux was enhanced with increasing
 96 DEA concentration, solution temperature and liquid velocity. In other works,⁴⁵ wet spun
 97 polyetherimide (PEI) membrane blended with polyethylene glycol (PEG) was developed to
 98 evaluate the effect of various PEI concentrations (13-16 wt %) on CO₂ stripping performance
 99 from DEA solution. It was found that the membrane produced with 14 wt% PEI concentration
 100 achieved the maximum CO₂ flux of 2.7×10^{-2} (mol/m².s).

101

102 Despite the above mentioned researches on stripping applications, to our knowledge, no
 103 research has been conducted thus far into the effect of SMM migration to the HF membrane
 104 surface on CO₂ stripping flux from aqueous DEA solution and water. The first attempt is hence
 105 made in the present work to manufacture SMM blended PSf HFs with different air-gap distances,
 106 to characterize the HFs so manufactured by various methods and to investigate the performance
 107 of CO₂ stripping flux from DEA and water in a MC application.

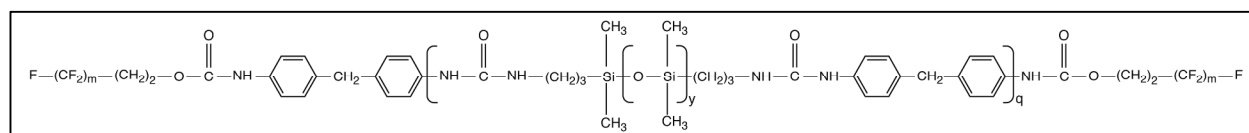
108 2. Experimental

109 2.1. HFM preparation

110 To prepare spinning dope 17 wt% PSf (Udel P-1700, from Solvay Advance Polymer) and 1
 111 wt% laboratory synthesized SMM was mixed in N-methyl-2-pyrrolidone (NMP>99.5%,
 112 purchased from Merck) by mechanical stirring at 60 °C to achieve a stable and uniform solution.

113 Fig. 1 shows the SMM structure, where *m* represents the repeating units of CF₂ and equals to
 114 7.58, *y* indicates a,*o*-aminopropyl poly (dimethyl siloxane) (PDMS) repeating units and is equal
 115 to 9.81 and *q* reveals repeating unit of urea and equals to 10.14. The detailed descriptions of
 116 SMM synthesis were given in other literatures.²⁵

117



118

119 **Fig. 1:** Structure of SMM

120
 121 Aqueous solution of diethanolamine (DEA>99%,from Merck) was used as the liquid
 122 absorbent in MC application. The sweeping and feed gaswere pure N₂ and CO₂, respectively.
 123 After degassing the resulting mixture by the aid of ultrasonic water bath, the PSf HFs (M₁-M₇)
 124 were spun with air-gaps of 0, 5, 10, 15, 20, 30 and 50 cm, respectively, according to the method
 125 described earlier.⁴⁶ Table 1 gives the detailed dry-wet spinning conditions applied in this work. To
 126 completely remove the residue of the additive, solvent and any impurities, the spun HFswere
 127 soaked in tap water for 3 days, before being dried at room temperature.

128
 129

Table 1 Experimental spinning conditions

Dope extrusion rate (ml/min)	4.5
Composition of bore fluid	NMP/water (60/40)
Bore fluid rate (ml/min)	2.00
Coagulation medium	Tap water
Spinneret dimension, o.d./i.d (mm)	1.20/0.55
Air-gap (cm)	0, 5, 10, 15, 20, 30 and 50
Temperature of coagulant (°C)	25

130

131 2.2. Characterization of prepared HFMs

132 PSf membranes were subjected to various characterization methods, which meticulously
 133 detailed in our previous study.⁴⁴ To acquire the average pore radius and the effective surface
 134 porosity of the HFs, helium permeation experiment was conducted based on the method
 135 described in our earlier work.⁴⁴ Contact angle (CA) of the fiber's outer dry surface was measured to
 136 obtain information about surface hydrophobicity of the HFs. To determine the membrane's
 137 resistance to the wetting, liquid entry pressure for both water (LEP_w) and DEA (LEP_{DEA}) was
 138 measured.⁴⁴ LEPS are considered as the pressure at which the first droplet of liquid was
 139 perceived on the upper skin of the HFM. HF's overall porosity (ϵ_m) was obtained using
 140 gravimetric method. To evaluate HF's mechanical endurance, collapsing pressure of each HF was
 141 measured.⁴⁴ Scanning electron microscope (SEM, tabletop microscope, TM3000) was used to
 142 obtain images of HF's cross-section and outer skin. Roughness (R_a) was obtained by atomic

143 force microscopy (AFM) using AFM equipment (SPA 300 HV, Japan) by the method of
144 Khayet *et al.*⁴⁷

145

146 2.3. CO₂ stripping evaluation

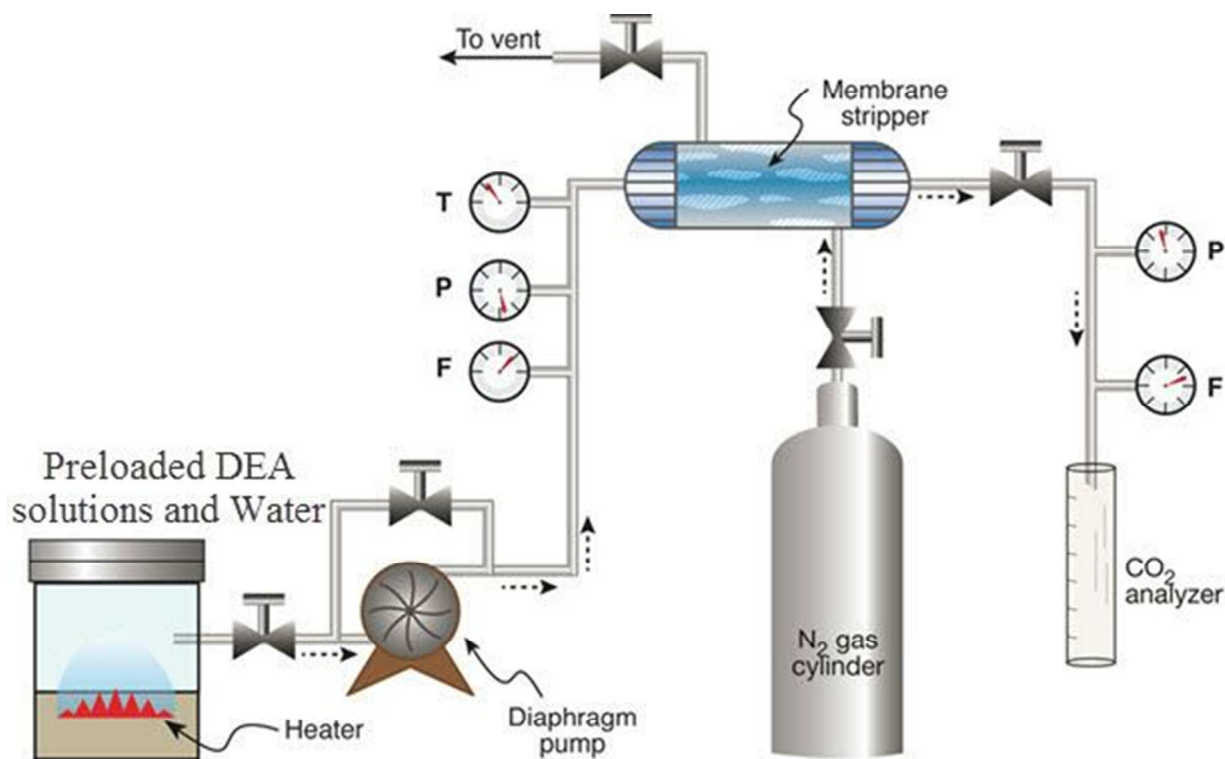
147 Fig. 2 indicates the experimental setup used for CO₂ stripping by the MC system. Thirty
148 HFs were assembled into bundles and placed in a stainless steel module which is specified in
149 details in Table 2. The aqueous DEA solution (1 DEA mol/L) or water was presaturated with
150 pure CO₂ up to 0.0006 mol/L, unless otherwise stated, and loaded in the feed reservoir. The CO₂
151 presaturated liquid and the stripping agent (pure N₂) flowed in the lumen and shell side of HFs,
152 respectively, in a counterflow mode. The calibrated flow meters were applied to regulate the
153 pressure and flow rate of the gas and liquid stream. In order to prohibit the bubble dispersion into
154 the liquid, the difference of 0.2×10^5 bar in pressure between N₂ and the liquid stream was applied.
155 The inlet and outlet CO₂ concentration in the liquid side was determined by the titration
156 method described in details by Li and Chang.⁴⁸

157 The flux of stripped CO₂ was obtained using the equation below:

$$158 J_{CO_2} = \frac{C_{l,i} - C_{l,o}}{A_i} \times Q_l \quad (1)$$

159 where J_{CO_2} is the flux of CO₂ stripped from liquid (mol/m².s), $C_{l,i}$ and $C_{l,o}$ indicate concentration
160 of CO₂ (mol/m³) in the liquid stream at the module inlet and outlet, respectively. Q_l is the liquid
161 flow rate (m³/s) and A_i is the HF inner surface (m²).⁴⁹

162



163

164 **Fig. 2** Experimental apparatus of stripping process via MC system.⁴⁹

165

166

167

168

169

Table 2 Specifics of MC module

Module i.d (mm)	14
Length of module (mm)	270
HF o.d (μm)	0.7-0.9
HF i.d (μm)	0.45-0.5
Effective length of HF (mm)	150
Number of HFs	30
Effective contact area (inner, mm^2)	6358.5

170

171

172

173 3. Results and Discussion

174 3.1. Structure of PSf membranes

175 The experimental findings of characterization tests are summarized in Table 3. From the
176 table the fiber's mean pore size was very large at the 30 and 50 cm air-gap, which is probably
177 ascribed to elongational effect. As well, the migration of a larger amount of SMM to the fiber
178 surface may also have contributed to pore size enlargement.

179
180 The enhancement of contact angle (CA) from $85.14 \pm 0.87^\circ$ to $93.01 \pm 0.93^\circ$ with increasing
181 air-gap up to 15 cm can be attributed to the presence of a larger amount of SMM at the HF
182 surface. On the other hand, a trend of decline in CA from 15 to 50 cm can be attributed to the
183 increased pore size for larger air-gaps. Notably, the increase of the pore size facilitates
184 penetration of water into the HF membrane pores, resulting in the reduction in CA values. According
185 to the AFM analysis the roughness of HF outside surface increased as the air gap increased from
186 0 to 50 cm, which may also have contributed to the enhancement of CA. Further increase in
187 roughness from the air gap of 15 to 50 cm is most likely associated with the increase in pore size,
188 which, as mentioned above has caused the decrease of CA. In any case, all HF surfaces exhibited
189 CA of higher than that of the plain dry spun PSf HF ($63 \pm 1.5^\circ$) by Rahbari-Sisakht *et al.*²⁴, which is
190 another evidence of the surface migration of hydrophobic SMM.

191
192 The collapsing pressure of PSf HF membranes has gradually increased as the air-gap
193 changed from 0 to 50 cm, which was mainly caused by interaction of base polymer with surface
194 migrated SMM.

195
196 The HF's overall porosities are considered to be high enough for MC due to the low
197 polymer concentration in the spinning solution. Furthermore, the surprising decrease of the overall
198 porosity decreased gradually with the increase in the air-gap, which is associated with the
199 reduced HF dimension (i.e., o.d and wall thickness) at the higher air-gaps. In addition, a parallel
200 relationship is found between CA and LEPw, i.e. both CA and LEPw increased up to 15 cm air-
201 gap, decreased a little from 15 to 20 cm and then increased continuously from 20 to 50 cm.
202 Hence, it can be concluded that LEPw was also influenced by both the pore size and the amount

203 of migrated SMM to the surface. M₄ membrane showed the highest resistance to the wetting for
 204 both water and aqueous DEA solution.

205

206

207

208 **Table 3** Experimental data of characterization tests for PSf HFs

HF Number	Air-gap distance (cm)	Average pore size (nm)	Effective surface porosity $\frac{\varepsilon}{L_p}$ (m ⁻¹)	LEP _w (×10 ⁵ pa)	LEP _{DEA} (×10 ⁵ pa) at 80 °C	CA (outer surface)	Collapsing pressure (×10 ⁵ pa)	Overall porosity (%)	Roughness (<i>R_a</i>)
M ₁	0	108.95	2.00	5.00±0.72	4.5±0.25	85.14±0.87	7	70	4.12
M ₂	5	141.18	1.97	5.00±1.32	4.5±0.68	85.81±1.46	7.5	70	4.85
M ₃	10	88.61	3.84	5.00±0.40	4.00±1.40	87.23±1.23	8	69	5.54
M ₄	15	21.27	33.28	5.5±0.64	5.00±0.25	93.01±0.93	8.5	68	6.41
M ₅	20	62.96	11.40	3.5±1.07	3.00±0.50	88.80±1.37	8.5	68	7.31
M ₆	30	257.70	3.10	4±0.82	3.50±1.25	90.00±1.07	9	66	8.06
M ₇	50	774.83	0.34	4.5±0.53	3.50±0.50	91.78±1.29	9	58	8.58

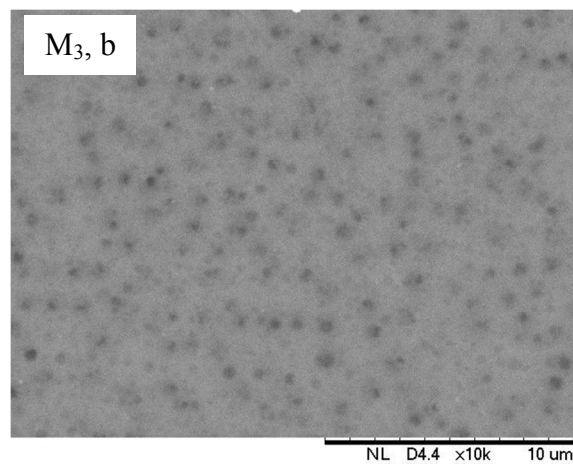
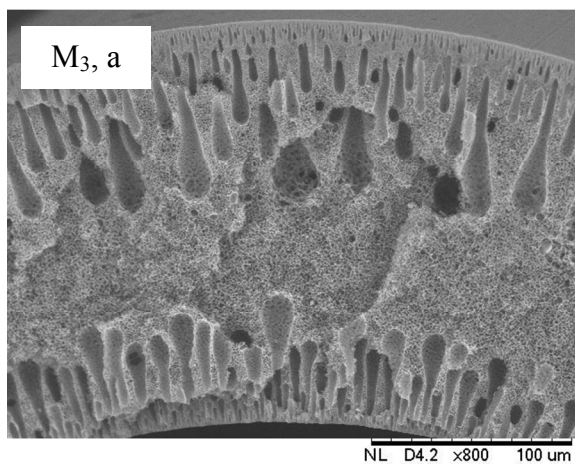
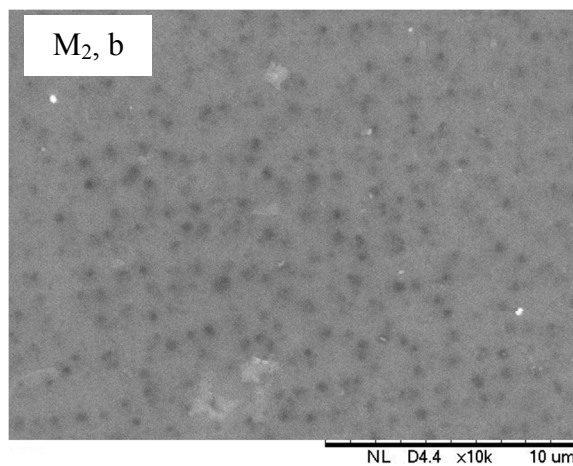
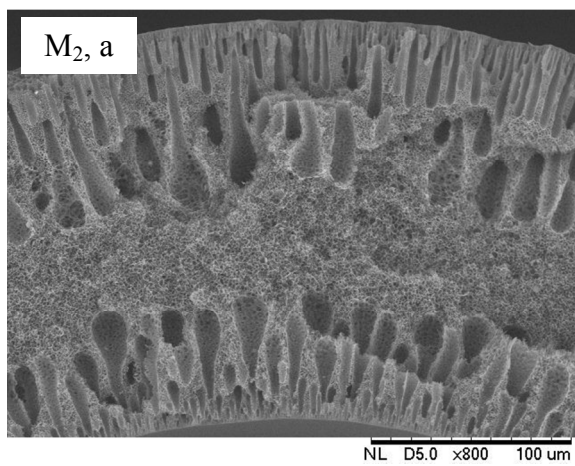
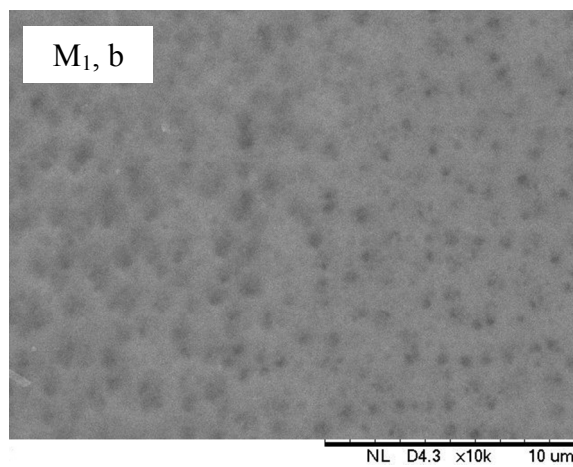
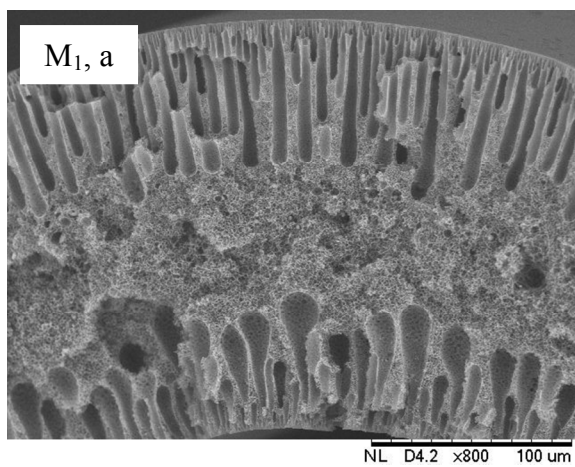
209

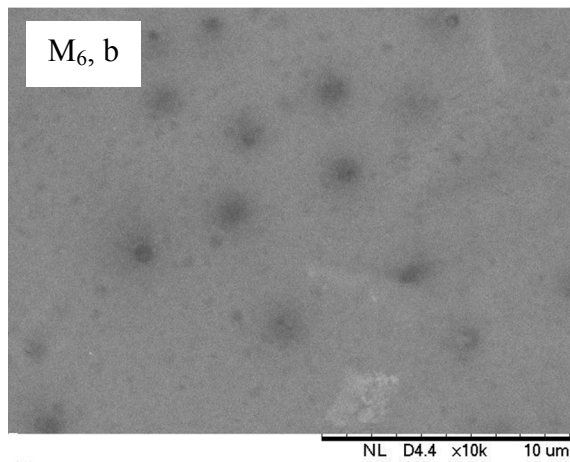
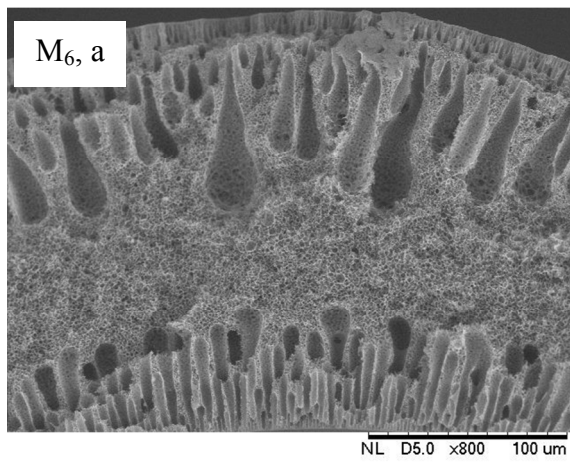
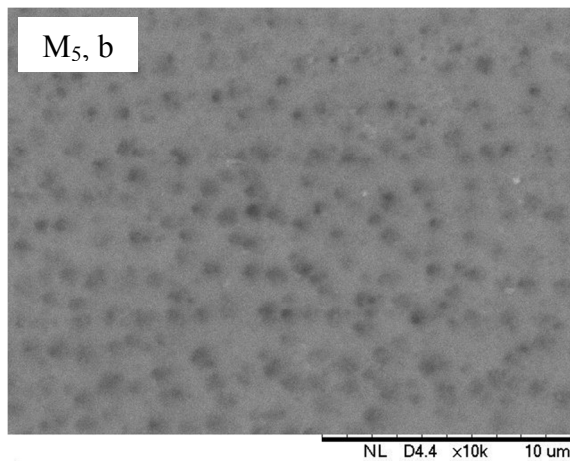
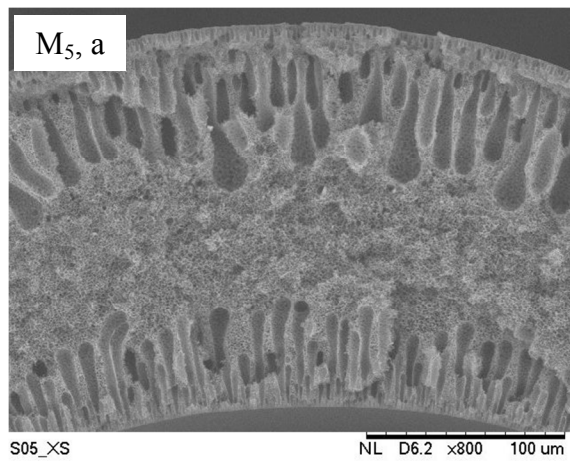
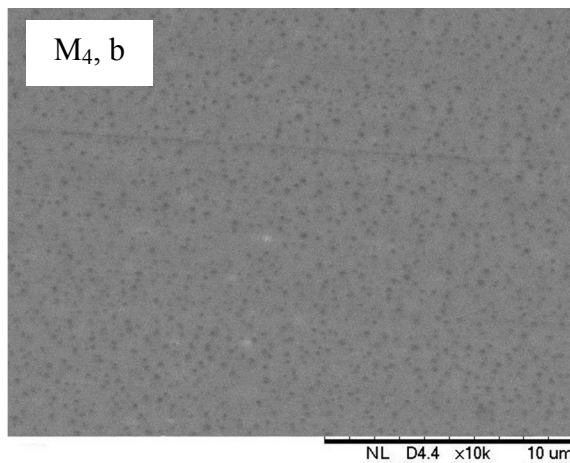
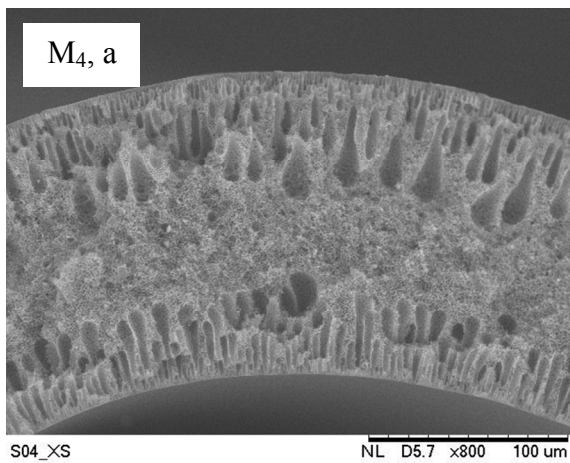
210

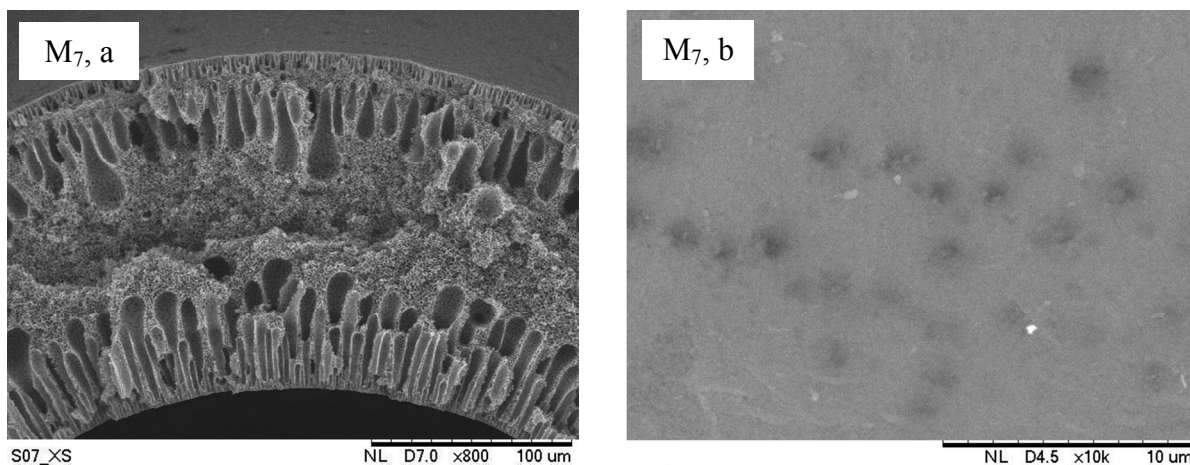
211

212 3.2. SEM observation

213 Fig. 3 displays the SEM images of the HF's cross-section and the outer skin surface for
 214 air-gaps ranging from 0 to 50 cm. The HF diameters declined from 952 to 654 μm (o.d) and
 215 from 604 to 460 μm (i.d), respectively, as the air-gap changed from 0 to 50 cm due to HF
 216 elongation. All HFs have porous skin layers on both inner and outer surfaces. Finger-like voids
 217 extended from both sides to the middle section of the HF. As shown in Fig. 3 the size of the
 218 macrovoids in the HF lumen side became larger as the air-gap length increased, which can be
 219 ascribed to the more contact time of the spun HF with the inner coagulant.







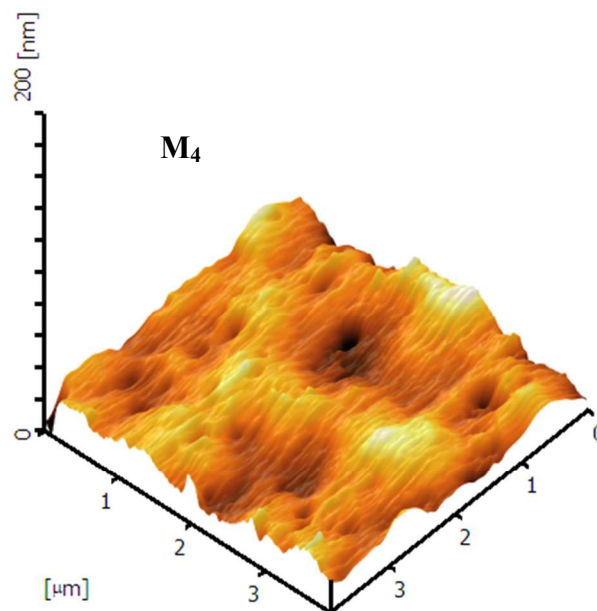
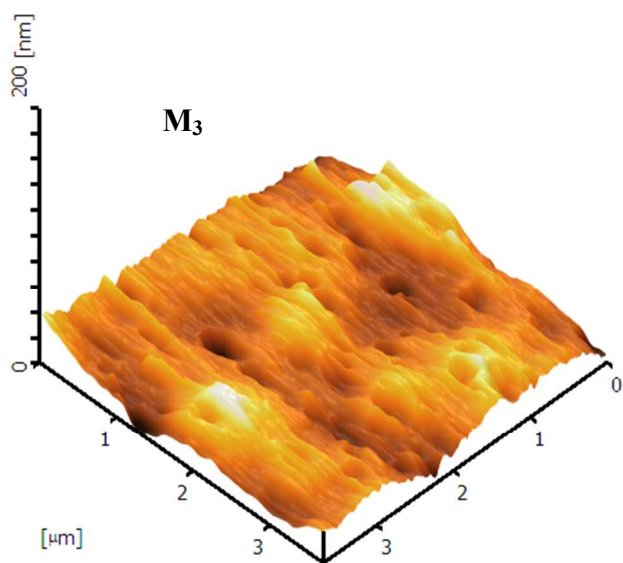
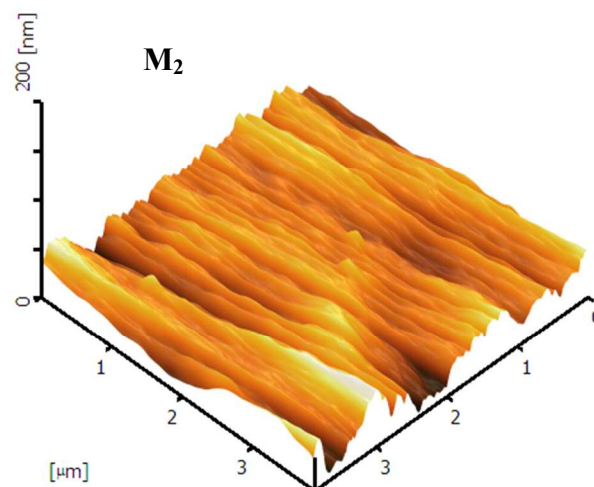
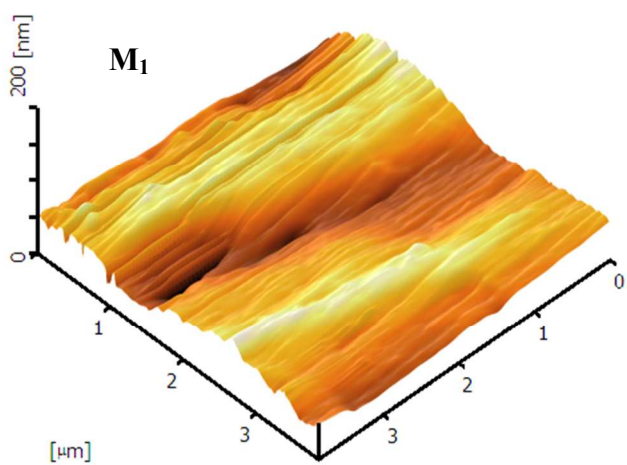
220 **Fig. 3** SEM images of the PSF hollow fibers (a) cross-section, (b) outer surface.

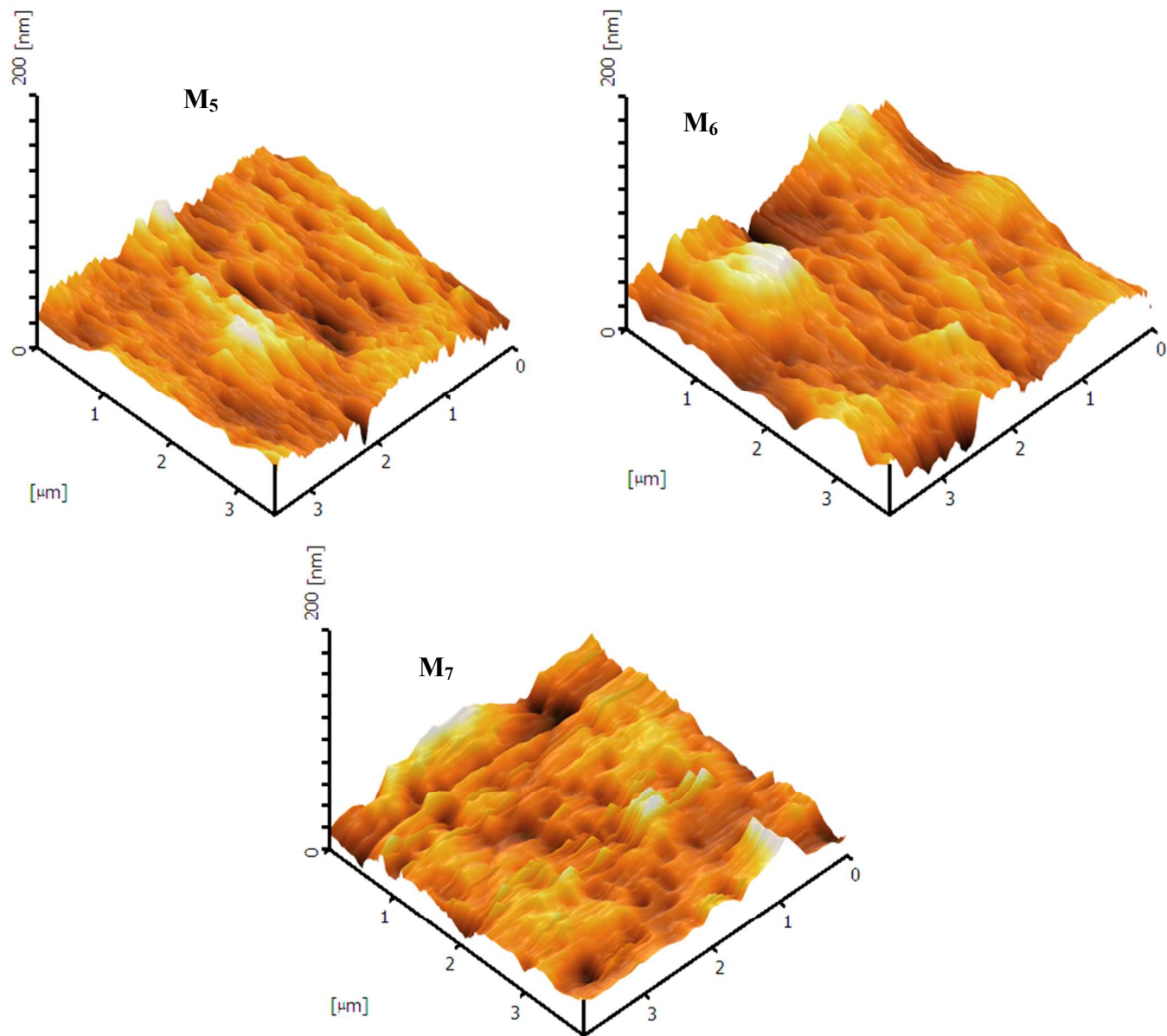
221

222

223 3.3. AFM analysis

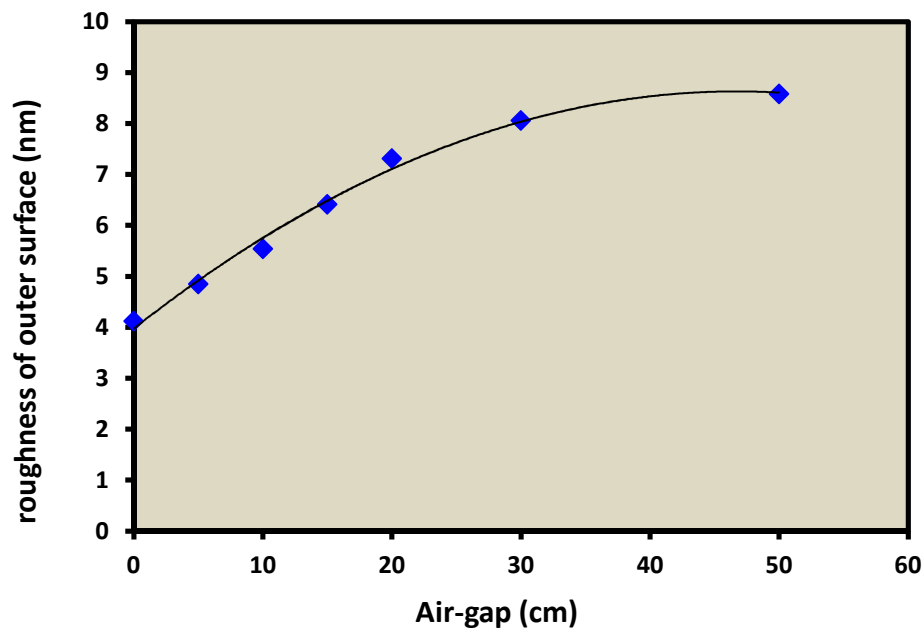
224 Fig. 4 shows the 3D AFM micrographs of the HF's outer surface. The roughness of the
225 HF's (M_1 - M_7) outer surface increases gradually with an increase in air-gap, as it is quantitatively
226 shown in Fig. 5. The similar morphological behaviour was observed for surface modified
227 polyethersulfone (PES) membranes spun with various air-gaps of 50 to 90 cm, which was
228 attributed to the presence of larger amount of SMM at the HF surface.⁵⁰ It is noteworthy that the
229 parallel nodular alignment is obvious for short air-gaps and it becomes more obscure as the air-
230 gap increases. It is likely because of polymer relaxation that occurs while the pristine HF is
231 traveling through the air-gap.





232

Fig. 4 AFM 3D micrographs of the PSf hollow fibers (outer surface).



233

234

Fig. 5 Roughness parameter of HF's outer surface vs. air-gap length.

235

236

3.4. CO₂ stripping evaluation results

237

Fig. 6 illustrates the influence of liquid (1 mol/L, DEA) velocity on stripping flux at the

liquid temperature of 80 °C. The figure shows an increasing trend in stripping flux as DEA

velocity increases, which confirms the decreased resistance of liquid phase boundary layer.⁵¹ A

maximum stripping flux of 4.50×10^{-2} (mol/m².s) was achieved by HF M₄ at DEA velocity of 0.7

(m/s). A similar behavior can be seen by Fig. 7 when the liquid absorbent is water.

242

The membrane that has been fabricated using 15 cm air gap length (M₄) is unique in many

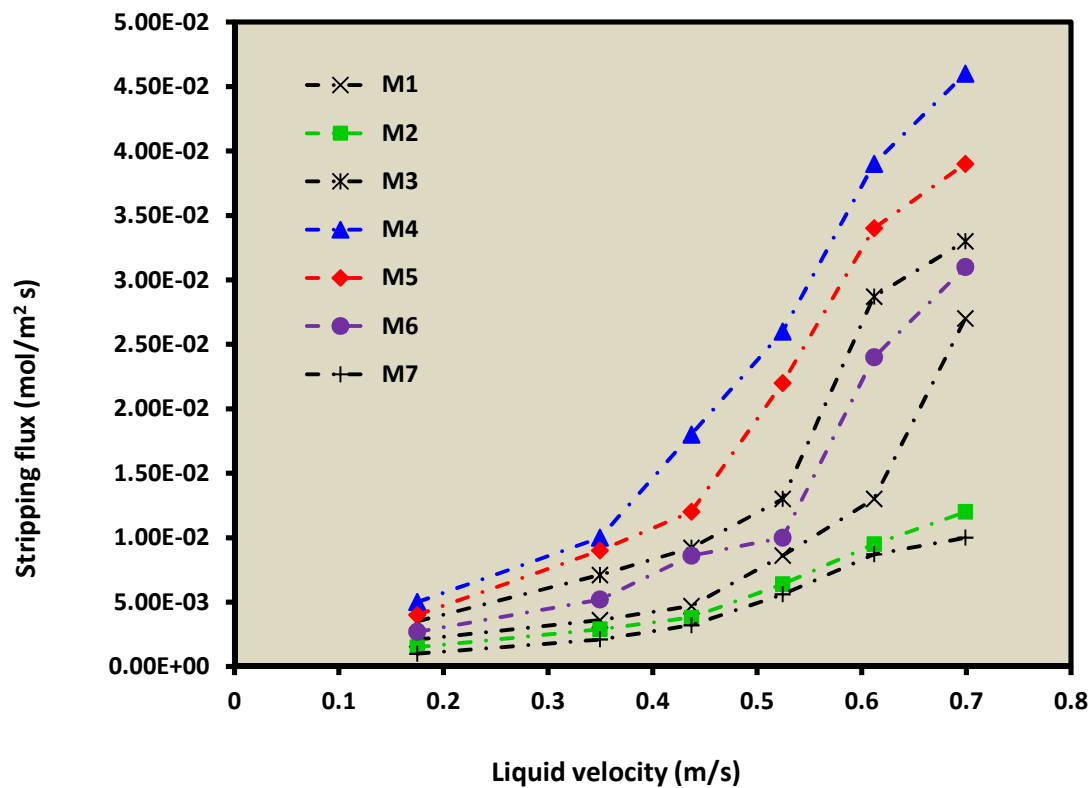
aspects among all the studied HFs. In particular, M₄ has the highest effective surface porosity

(see Table 3), enabling the fastest gas transport due either to the large surface porosity or to the

small effective membrane thickness. Its LEP_w is also the highest due to the smallest pore size

and the highest contact angle. Thus, M₄ has all the desirable features of MC applications.

247



248

249 **Fig. 6** CO₂ stripping flux vs. liquid velocity (DEA solution). ($T_{\text{DEA}}=80$ °C, $M_{\text{DEA}}=1$ mol/L, gas
250 flowrate=50 ml/min).

251

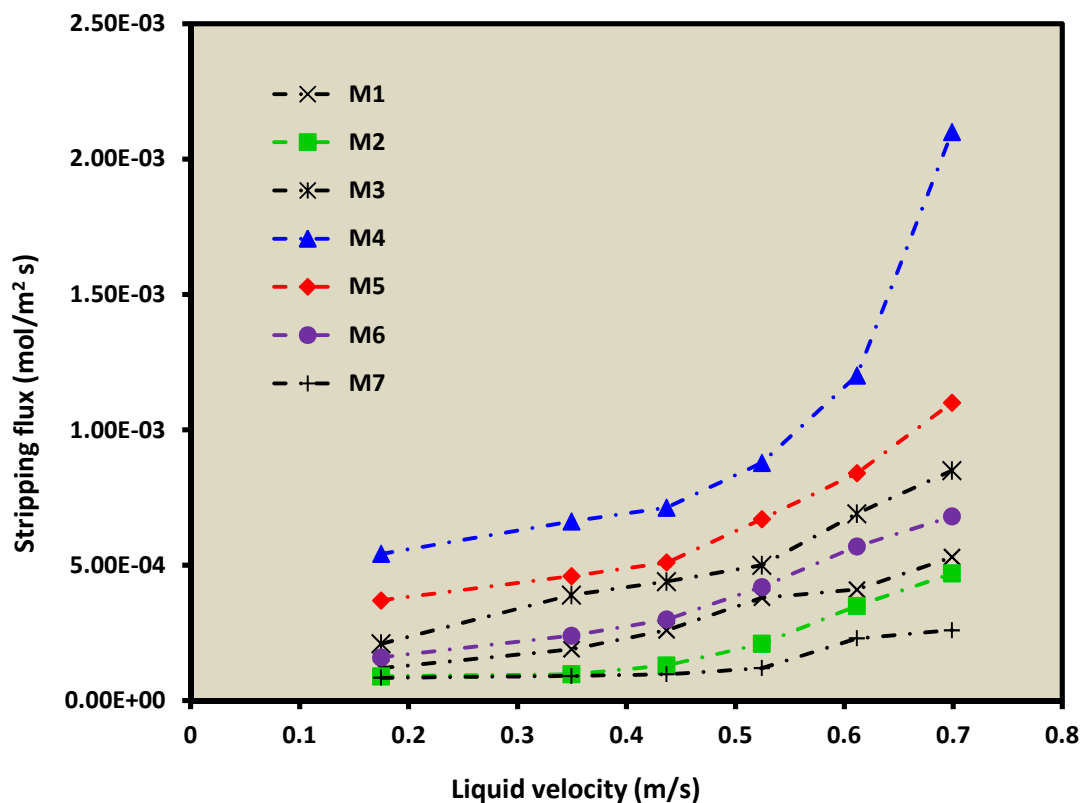
252

253

254

255

256



257
258 **Fig. 7** CO₂ stripping flux vs. liquid velocity (water). (T=80 °C, gas flow rate = 50 ml/min).

259
260 In Table 4 and 5 comparisons were made between the CO₂ stripping fluxes from aqueous
261 DEA solution and water, respectively, of the membranes fabricated in this work and those
262 reported in other studies.^{44,52-55} The velocity of both DEA solution and water flow was
263 maintained at 0.7 m/s. As the tables show, M₄ membrane fabricated in this work at 15 cm air-gap
264 and modified with 1wt% SMM, shows the best CO₂ fluxes.

265
266
267
268
269
270
271
272
273

274 **Table 4** Results of CO₂ stripping flux from DEA solution for different HFs

Membrane	Polymer material	Air-gap (cm)	Additive	CO ₂ flux (mol/m ² .s)	Reference	Liquid absorbent
M ₁	PSf	0	1wt%SMM	2.70×10 ⁻²	This work	DEA
M ₂	PSf	5	1wt% SMM	1.20×10 ⁻²	This work	DEA
M ₃	PSf	10	1wt% SMM	3.30×10 ⁻²	This work	DEA
M ₄	PSf	15	1wt% SMM	4.60×10 ⁻²	This work	DEA
M ₅	PSf	20	1wt% SMM	3.90×10 ⁻²	This work	DEA
M ₆	PSf	30	1wt% SMM	3.10×10 ⁻²	This work	DEA
M ₇	PSf	50	1wt% SMM	1.00×10 ⁻²	This work	DEA
-	PVDF	5	1wt% SMM	1.20×10 ⁻³	[44]	DEA
-	PVDF	0	-	2.20×10 ⁻²	[55]	DEA
-	PVDF	0	5wt% PEG	3.70×10 ⁻²	[55]	DEA
-	PVDF	0	5wt% glycerol	2.00×10 ⁻²	[53]	DEA
-	PVDF	0	5wt% LiCl	3.75×10 ⁻²	[53]	DEA
-	PVDF	0	5wt% methanol	2.60×10 ⁻²	[53]	DEA
-	PVDF	0	5wt% phosphoric acid	2.70×10 ⁻²	[53]	DEA
-	PVDF	0	-	2.70×10 ⁻²	[53]	DEA
-	PEI	0	-	9.00×10 ⁻³	[55]	DEA
-	PEI	0	5wt% PEG	2.35×10 ⁻²	[55]	DEA

275

276

277

278

279

280

281

282

283

284

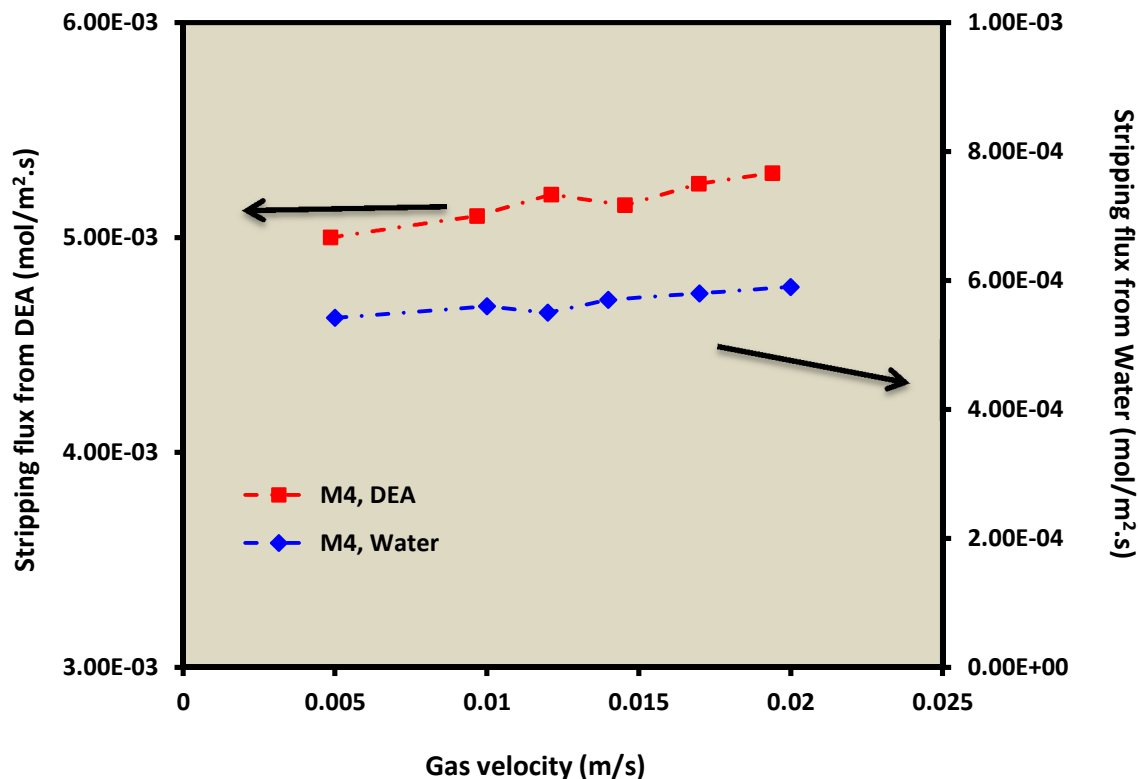
285

286 **Table 5** Results of CO₂ stripping from water for different membranes

Membrane	Polymer material	Air-gap (cm)	Additive	CO ₂ flux (mol/m ² .s)	Reference	Liquid absorbent
M ₁	PSf	0	1wt% SMM	5.30×10 ⁻⁴	This work	Water
M ₂	PSf	5	1wt% SMM	4.70×10 ⁻⁴	This work	Water
M ₃	PSf	10	1wt% SMM	8.50×10 ⁻⁴	This work	Water
M ₄	PSf	15	1wt% SMM	2.10×10 ⁻³	This work	Water
M ₅	PSf	20	1wt% SMM	1.10×10 ⁻³	This work	Water
M ₆	PSf	30	1wt% SMM	6.80×10 ⁻⁴	This work	Water
M ₇	PSf	50	1wt% SMM	2.60×10 ⁻⁴	This work	Water
-	PSf	0	4wt% glycerol	1.30×10 ⁻⁴	[54]	Water
-	PVDF	0	5wt% glycerol	1.90×10 ⁻³	[52]	Water

287

288 Fig. 8 demonstrates the relationship between gas velocity and stripping flux for both
 289 DEA solution and water. The results for M₄ membrane (15 cm air-gap) are plotted in the figure,
 290 but all other HFs would show a similar trend. As shown in Fig. 8, no noticeable stripping flux
 291 was perceived as the gas velocity was varied from 0.005 to 0.002 (m/s). This finding perfectly
 292 validates interpretations by Khaisri *et al.* that the liquid phase primarily governs mass transfer
 293 rate of MC stripping and the mass transfer resistance of gas stream has negligible effect on
 294 stripping flux.⁴⁰



295
 296 **Fig. 8** CO₂ stripping flux vs. gas velocity. ($T_{\text{DEA \& Water}}=80\text{ }^{\circ}\text{C}$, $M_{\text{DEA}}=1\text{ mol/L}$, liquid flow rate
 297 $=50\text{ mL/min}$).

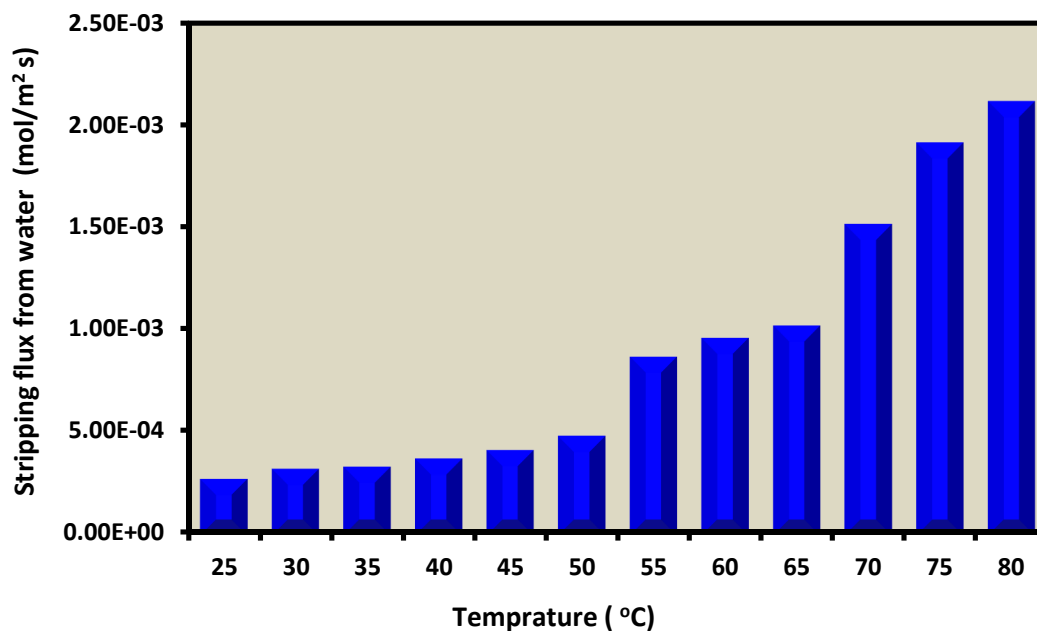
298
 299 The influence of liquid temperature on the stripping performance of M₄ membrane was
 300 also studied and the results for water and DEA solution in Fig.9 and 10, respectively. As shown
 301 in Fig. 9, a marked increase of stripping flux occurred from 2.50×10^{-4} to 4.60×10^{-2} (mol/m².s) as
 302 the temperature of water changed from 25°C to 80 °C, which can be attributed to the decrease of
 303 CO₂ solubility as the water temperature increases.^{44,54} Fig. 10 also shows that the stripping flux of
 304 CO₂ increased as the DEA temperature was increased from 25°C to 80 °C. It could be said that
 305 diffusion coefficient, equilibrium constant of chemical reaction and equilibrium partial pressure
 306 of CO₂ are strongly influenced by liquid temperature.⁴⁰ A decrease in equilibrium constant of the
 307 following reaction (equation 2) leads to enhancement of CO₂ partial pressure in the gas side by
 308 the factor of 5 to 8 as the temperature is increased by 10 °C.⁵⁶ Consequently, an increase in
 309 working temperature results in elevated driving force for CO₂ stripping from the DEA solution.

310



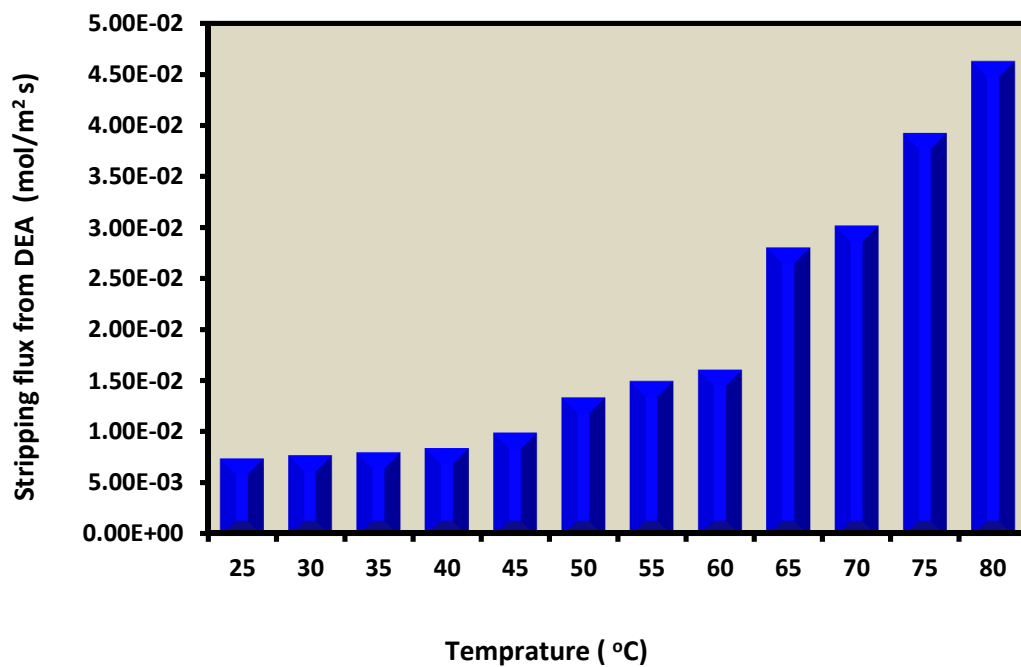
312

313



314

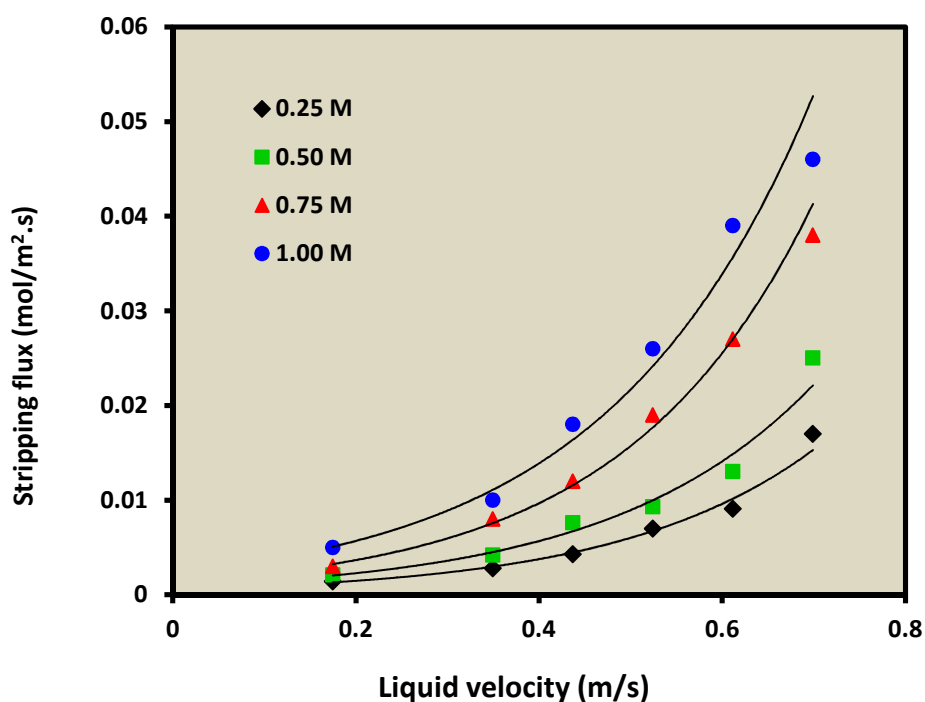
315 **Fig. 9** CO₂ stripping flux vs. liquid phase temperature (water) (liquid and gas flow rate = 200,
316 50 ml/min, respectively).



317

318 **Fig. 10** CO₂ stripping flux vs. liquid phase temperature (DEA) (liquid and gas flow rate = 200,
319 50 ml/min, respectively).

320 Fig.11 reveals the relationship between DEA concentration and stripping flux of M₄ HF
321 in the MC system. As illustrated in the figure an increase in DEA concentration from 0.25 to 1 M
322 results in elevation of stripping flux, which can be validated by the reaction represented by
323 equation 2. As it is interpreted by Rahbari-Sisakht *et al.*, increase of DEA concentration causes
324 enhancement of absorbed CO₂ during preloading in the form of R₂NCOO⁻ion.⁴⁴ During the
325 stripping procedure, release of CO₂ causes the elevated CO₂ partial pressure at the interface,
326 resulting in increase of driving force.⁴⁰
327



328
329 **Fig.11** CO₂ stripping flux vs. liquid velocity for various DEA concentration (gas flow rate =
330 50 ml/min, T=80 °C).

331
332
333
334 **4. Conclusion**
335
336 The SMM blended PSfHFs were spun with air-gaps of 0 to 50 cm and utilized to strip CO₂ by MC
337 from DEA solution and water. M₄ membrane that was spun at 15 cm air-gap showed the highest
338 stripping flux of 4.60×10^{-2} and 2.10×10^{-3} (mol/m².s) for DEA solution and water, respectively, at

339 the liquid velocity of 0.7 (m/s). Higher liquid velocities significantly increased stripping
340 flux; however gas velocity exerted no significant influence, corroborating that liquid boundary
341 resistance is predominant. Additionally, it was found that the change in liquid temperature from
342 25°C to 80 °C increased the stripping flux from 2.50×10^{-4} to 2.10×10^{-3} mol/m².s and 7.10×10^{-3} to
343 4.60×10^{-2} mol/m².s, for water and DEA solution, respectively. Increasing the DEA concentration
344 from 0.25 to 1 mol/L, resulted in elevation of stripping flux from 1.70×10^{-2} to 4.60×10^{-2}
345 (mol/m².s) at DEA velocity of 0.7 m/s. Based on the experimental results, the data obtained
346 from the HF spun at the optimum air-gap length (15 cm) surpassed the stripping flux data reported
347 in other studies.

348

349

350

351 References

- 352 1 T.C. Merkel, H. Lin, X. Wei and R. Baker, *J. Membr. Sci.*, 2010, 359, 126–139.
- 353 2 W.J. Koros and G.K. Fleming, *J. Membr. Sci.*, 1993, 83, 1-80.
- 354 3 X.Y. Chen, H. Vinh-Thang, D. Rodrigue and S. Kaliaguine, *RSC Adv.*, 2014, 4, 12235-
355 12244.
- 356 4 S. Danaei Kenarsari, D. Yang, G. Jiang, S. Zhang, J. Wang, A.G. Russell, Q. Wei
357 and M. Fan, *RSC Adv.*, 2013, 3, 22739-22773.
- 358 5 R.W. Baker, *Ind. Eng. Chem. Res.*, 2002, 41, 1393–1411.
- 359 6 J. Lu, L. Wang, X. Sun, J. Li and X. Liu, *Ind. Eng. Chem. Res.*, 2005, 44, 9230-9238.
- 360 7 M.G. Buonomenna, W. Yave and G. Golemme, *RSC Adv.*, 2012, 2, 10745–10773.
- 361 8 D. deMontigny, P. Tontiwachwuthikul and A. Chakma, *Ind. Eng. Chem. Res.*, 2005, 44,
362 5726-5732.
- 363 9 Z. Wang, M. Fang, H. Yu, C.-C. Wei and Z. Luo., *Ind. Eng. Chem., Res.* 2013, 52,
364 18059–18070.
- 365 10 M.S. Abd Rahaman, L. Zhang, L.-H. Cheng, X.-H. Xu and H.-L. Chen, *RSC Adv.*, 2012, 2,
366 9165–9172.
- 367 11 Y.-F. Lin, C.-C. K, C.-H. Chen, K.-L. Tung and K.-S. Chang, *RSC Adv.*, 2014, 4, 1456-
368 1459.
- 369 12 P.H.M. Feron and A.E. Jesen, *Sep. Purif. Technol.*, 2002, 27, 231-242.

- 370 13 V.Y. Dindore, D.W.F. Brillman, P.H.M. Feron and G.F. Versteeg, *J. Membr.*
371 *Sci.*,2004.,235(1-2), 99-109.
- 372 14 R. Wang, H.Y. Zhang, P.H.M. Feron and D.T. Liang, *Sep. Purif. Techno.*, 2005, 146, 33-
373 40.
- 374 15 A.L. Ahmad, A.R., Sunarti, K.T. Lee and W.J.N. Fernando, *Int. J. Greenhouse Gas*
375 *Control.*, 2010, 4, 495-498.
- 376 16 A. Mansourizadeh and A.F. Ismail, *Int. J. Greenhouse Gas Control.*, 2011a, 5, 374-380.
- 377 17 P. Luis, B. Vander Bruggen and T. Van Gerven, *J. Chem. Technol. Biotechno.*, 2011, 186,
378 769-775.
- 379 18 M. Rahbari-Sisakht, A.F. Ismail, D. Rana and T. Matsuura, *Sep. Purif. Technol.*, 2012a, 98,
380 472-480.
- 381 19 M.Rahbari-Sisakht, A.F. Ismail, and T. Matsuura, *Sep. Purif. Technol.*, 2012b, 86, 215-
382 220.
- 383 20 Mansourizadeh, A., Z. Aslmahdavi, A.F. Ismail and Matsuura, T, *Int. J. Greenhouse Gas*
384 *Control.*,2014, 26, 83-92.
- 385 21 M. Rezaei, A.F. Ismail, S. A. Hashemifard, Gh. Bakeri and T. Matsuura, *Int. J.*
386 *Greenhouse Gas Control.*, 2014, 26, 147-157.
- 387 22 M. Rahbari-sisakht, A.F. Ismail and T. Matsuura, *Sep. Purif. Technol.*, 2012c, 88, 99-106.
- 388 23 D. E. Suk, G. Chowdhury, T. Matsuura, R. M. Narbaitz, P. Santerre, G. Pleizier and Y.
389 Deslandes, *Macromolecules* , 2002, 35, 3017-3021.
- 390 24 M. Rahbari-Sisakht, A.F. Ismail, D. Rana and T. Matsuura, *Sep. Purif. Technol.*, 2012d,
391 99, 61-68.
- 392 25 D.E. Suk, T. Matsuura, H.B. Park and Y.M. Lee, *J. Membr. Sci.*, 2006, 277, 177-185.
- 393 26 T.S. Chung and X. Hu, *J. Appl. Polym. Sci.*, 1997, 66, 1067-1077.
- 394 27 D. Wang, K. Li and W.K. Teo, *J. Membr. Sci.*, 1998, 138, 193-201.
- 395 28 D. Wang, K. Li and W.K. Teo, *J. Membr. Sci.*, 1999, 163, 211-220.
- 396 29 D. Wang, K. Li and W.K. Teo, *J. Membr. Sci.*, 2000, 176, 147-158.
- 397 30 J.-J. Qin, J. Gu and T.-S. Chung, *J. Membr. Sci.*, 2001, 182, 57-75.
- 398 31 G.C. Kapantaidakis, G.H. Koops and M. Wessling, *Desalination.*, 2002, 144, 121-125.
- 399 32 H.A. Tsai, D.H. Huang, S.C. Fan, Y.C. Wang, C.L. Li and K.R. Lee, *J. Membr. Sci.*, 2002,
400 198, 245-258.

- 401 33 M. Khayet, *Chem. Eng. Sci.*, 2003, 58, 3091-3104.
- 402 34 K.C. Khulbe, C.Y. Feng, F., Hamad, T. Matsuura and M. Khayet, *J. Membr. Sci.*, 2004, 245,
403 191-198.
- 404 35 x. Zhang, Y. Wen, Y. Yang and L. Liu, *J. Membr. Sci.*, 2008, 47, 1039-1046.
- 405 36 M. Khayet, M.C. García-Payo, F.A. Qusay and M.A. Zubaidy, *J. Membr. Sci.*, 2009, 330,
406 30-39.
- 407 37 S.-H. Yeon, K.-S. Lee, B., Sea, Y.-I. Park and K.-H. Lee, *J. Membr. Sci.*, 2005, 257, 156-
408 160.
- 409 38 A. Mansourizadeh, A.F. Ismail, M.S. Abdullah and B.C. Ng, *J. Membr. Sci.*, 2010, 355,
410 200-207.
- 411 39 H.B. Al-saffar, B. Ozturk and R. Hughes, *Chem. Eng. Res. Des.*, 1997, 75, 685-692.
- 412 40 S. Khaisri, D. deMontigny, P. Tontiwachwuthikul and R. Jiraratananon, *J. Membr. Sci.*,
413 2011, 376, 110-118.
- 414 41 H. Kumazawa, *Chem. Eng. Commun.*, 2000, 182, 163-179.
- 415 42 R. Naim, A.F. Ismail and A. Mansourizadeh, *J. Membr. Sci.*, 2012a, 392-393, 29-37.
- 416 43 A. Mansourizadeh and A.F. Ismail, *Desalination.*, 2011b, 273, 386-390.
- 417 44 M. Rahbari-Sisakht, A. F. Ismail, D. Rana, and T. Matsuura, *J. Membr. Sci.*, 2013a, 427,
418 270-275.
- 419 45 R. Naim and A.F. Ismail, *J Hazard Mater.*, 2013, 250-251, 354-361.
- 420 46 A.F. Ismail, I.R. Dunkin, S.L. Gallivan and S.J. Shilton, *Polymer.*, 1999, 40, 6499-6506.
- 421 47 M. Khayet, C.Y.K. Feng, C. Khulbe and T. Matsuura, *Desalination.*, 2002, 148, 321-327.
- 422 48 M. Li and B.-C. Chang, *J. Chem. Eng. Data.*, 1994, 39, 448-452.
- 423 49 M. Rahbari-Sisakht, D. Rana, T. Matsuura, D. Emadzadeh, M. Padaki and A.F. Ismail,
424 *Chem. Eng. J.*, 2014, 246, 306-310.
- 425 50 K.C. Khulbe, C.Y. Feng, T. Matsuura, D.C. Mosqueda-Jimenez, M. Rafat, D. Kingston,
426 R.M. Narbaitz and M. Khayet, *J. Appl. Polym. Sci.*, 2007, 104, 710-721.
- 427 51 M. Simioni, S.E. Kentish and G.W. Stevens, *J. Membr. Sci.*, 2011, 378, 18-27.
- 428 52 A. Mansourizadeh, *Eng. Res. Des.*, 2012, 90, 555-562.
- 429 53 R. Naim, A.F. Ismail and A. Mansourizadeh, *J. Membr. Sci.*, 2012b, 423-424, 503-513.
- 430 54 M. Rahbari-Sisakht, A.F. Ismail, D. Rana, T. Matsuura and D. Emadzadeh, *Sep. Purif.*
431 *Technol.* 2013b, 108, 119-123.

432 55 R. Naim, A.F. Ismail, N.B. Cheer and M.S. Abdullah, *Chem, Eng. Res. Des.*, 2014, 92,
433 1391-1398.

434 56 R.H., Weiland, M. Rawal and R.G. Rice, *AIChE J.*, 1982, 28, 963–973.

435

436

437

438

439

440

441

442

443

444

445

446

447

448

449

450

451

452

453

454

455

456 **List of Tables**457 **Table 1** Experimental spinning conditions458 **Table 2** Specifics of MC module459 **Table 3** Experimental data of charecterization testsfor PSf HF's460 **Table 4** Results of CO₂ stripping flux from DEA solution for different HF's461 **Table 5** Results of CO₂ stripping from water for different membranes

462

463

464 **List of Figures**465 **Fig. 1** Structure of SMM466 **Fig. 2** Experimental apparatus of stripping process via MC system.467 **Fig. 3** SEM images of the PSFhollow fibers (a) cross-section, (b) outer surface.468 **Fig. 4** AFM 3D micrographs of the PSf hollow fibers (outer surface).469 **Fig. 5** Roughness parameter of HF's outer surface vs. air-gap length.470 **Fig. 6** CO₂ stripping flux vs. liquid velocity (DEA solution). ($T_{\text{DEA}}=80\text{ }^{\circ}\text{C}$, $M_{\text{DEA}}=1\text{ mol/L}$, gas
471 flowrate =50 ml/min).472 **Fig. 7** CO₂ stripping flux vs. liquid velocity (water). ($T=80\text{ }^{\circ}\text{C}$, gas flow rate = 50 ml/min).473 **Fig. 8** CO₂ stripping flux vs. gas velocity. ($T_{\text{DEA}\&\text{ Water}}=80\text{ }^{\circ}\text{C}$, $M_{\text{DEA}}=1\text{ mol/L}$, liquid flow rate
474 = 50 mL/min).475 **Fig. 9** CO₂ stripping flux vs. liquid phase temperature (water) (liquid and gas flow rate = 200,
476 50 ml/min, respectively).477 **Fig. 10** CO₂ stripping flux vs. liquid phase temperature (DEA) (liquid and gas flow rate = 200,
478 50 ml/min, respectively).479 **Fig. 11** CO₂ stripping flux vs. liquid velocity for various DEA concentration (gas flow rate =
480 50 ml/min, $T=80\text{ }^{\circ}\text{C}$).

481

482

RSC Advances Accepted Manuscript